land

MDPI

Article

Multi-Scenario Simulation Analysis of Land Use and Carbon Storage Changes in Changchun City Based on FLUS and InVEST Model

Yingxue Li, Zhaoshun Liu, Shujie Li * and Xiang Li

College of Earth Sciences, Jilin University, Changchun 130061, China; yingxue21@mails.jlu.edu.cn (Y.L.); zhaoshun@jlu.edu.cn (Z.L.); li_xiang21@mails.jlu.edu.cn (X.L.)
* Correspondence: lisj@jlu.edu.cn

Abstract: Land use change is an important reason for changes in carbon storage in terrestrial ecosystems. Therefore, analyzing the impact of land use change on carbon storage is important for exploring the sustainable development of cities and improving the value of ecosystem services. Taking Changchun City in the northeast of China as the research area, this paper simulates land use patterns under three scenarios up to 2030 using the FLUS model and assesses carbon storage from 2010 to 2030 using the InVEST model. It estimates the impact of land use change on carbon storage under several scenarios in Changchun. The results show that cultivated land plays an important role in carbon storage in Changchun. The transfer of cultivated land to construction land has been the main land use type conversion over the past decade, which has led to most of the carbon storage loss. In the natural growth scenario, the carbon storage would decline further. In the cultivated land protection scenario, meanwhile, this situation would be greatly improved. In the ecological protection scenario, the carbon storage would be increased due to the protection of ecological land. In the future, we should protect existing resources while simultaneously comprehensively improving the economic, social, and ecological benefits of the land.

Keywords: land use; FLUS model; InVEST model; carbon storage; scenario simulation

Citation: Li, Y.; Liu, Z.; Li, S.; Li, X. Multi-Scenario Simulation Analysis of Land Use and Carbon Storage Changes in Changchun City Based on FLUS and InVEST Model. *Land* **2022**, *11*, 647. https://doi.org/10.3390/land11050647

Academic Editor: Shaojian Wang

Received: 27 March 2022
Accepted: 25 April 2022
Published: 27 April 2022

1. Introduction

Global climate change threatens sustainable human development. Carbon storage, which is of great significance to mitigating global climate change, is one of the most important functional indicators of ecosystem services and a direct manifestation of terrestrial ecosystem productivity. It is an important index for measuring the scale and quantity of the primary productivity of an ecosystem [1]. Land use/cover change (LUCC) is an important cause of changes in carbon storage in terrestrial ecosystems. Human activities affect the carbon sequestration capacity of vegetation and soil by changing land cover or land use patterns, resulting in the degradation and change of ecosystem service functions. It has led to the imbalance of the global carbon cycle and a series of global environmental problems, including global warming and a sharp decline in biodiversity. Therefore, analyzing the impact of land use change on carbon storage is important for achieving sustainable urban growth and improving ecosystem service value.

With the increase in global warming, growing attention is being paid to the impact of land use change on carbon storage in the field of climate change research [2]. Scholars have simulated land use scenarios and carbon storage changes in the future based on various models that allow the prediction results to be visualized from different perspectives and at different scales. At the national scale, Liu et al. [3] analyzed the terrestrial carbon budget of the conterminous United States by integrating fine-scale processes including land use and land cover change into a large-scale ecosystem framework. They believed that most of the increase in carbon in the net primary productivity of ecosystems was offset

by increased carbon losses caused by farming and natural disturbances. Mendoza et al. [4] predicted land cover and carbon storage changes in Mexico up to 2050 under representative concentration pathways (RCPs) and shared socioeconomic pathways (SSPs), arguing that the ecosystems with the highest aboveground biomass (AGB) densities are cloud, tropical evergreen, and temperate forests, in contrast with scrublands and grasslands, which showed the lowest values. Liu et al. [5] assessed the impact of projected land use change on terrestrial carbon storage in China with the FLUS–InVEST model and came to the conclusion that carbon storage in the forests will continue to increase but will decreased in grassland in the RCPs scenario. Eigenbrod et al. [6] analyzed the spatiotemporal changes in carbon storage according to the simulations of urbanization and consequent land use change in Britain. The results indicated that Britain would experience different degrees of decline in carbon storage.

At the regional scale, Chinese scholars prefer to simulate the spatial distribution of carbon storage under different scenarios in basin and oasis ecosystems, such as the Yanqi oasis [7], the Shule River Basin [8], the Yili valley [9], and the Qi River Basin [1]. The conclusions of these studies agree that carbon storage decreases with land use change, especially if it involves the retreat of forest and grassland. As for urban ecosystems, case studies have been conducted focused on Zichang [10], Wuhan [11,12], Beijing [13], and Guangzhou [14], which all came to the same conclusion that carbon storage will decrease in the case of future urban expansion. Some researchers have suggested that changes in land use type due to increased cultivated land may increase carbon storage [15], while others have indicated that the trend of carbon storage will inevitably decline as a whole [16]. Li found that comprehensive spatial management could alleviate the contradiction between urban construction and environmental protection [12]. Carbon storage can be increased under the ecological protection scenario, but the reduction in the cultivated land area cannot be controlled effectively [17].

In terms of methodology, carbon storage is measured mainly by actual measurements or through the use of models. The carbon storage and sequestration module in the InVEST (Integrated Valuation of Ecosystem Services and Tradeoffs) model can evaluate the carbon storage over a period of time based on land use data and has the advantages of simple parameters and visualized results. For these reasons it has been widely used by scholars. As for simulating land use patterns, the Markov model is good at predicting quantities but struggles to represent them in space [18]. The Future Land Use Simulation model (FLUS) is based on the improvement of the cellular automata model to better simulate the spatial distribution of land types. It has been widely used in recent years in the field of land use simulation.

Nevertheless, there are few studies on the impact of urban land use change on carbon storage in the northeast of China. As the capital of Jilin Province, Changchun is at the center of the Northeast Asian Economic Circle and an important industrial base in China. With the proposal of the strategy of revitalizing the old industrial bases in northeast China, the urbanization and industrialization processes in Changchun City have accelerated substantially in recent decades. Rapid urbanization has led to a great loss of cultivated land, while compensation for the occupied cultivated land has resulted in further encroachment into ecological land [19,20], which has led to a large amount of carbon exchange. Based on the land use data of Changchun from 2010 to 2020, this paper projects the spatiotemporal change in carbon storage under three land use scenarios by 2030 (the natural growth (NG) scenario, the cultivated land protection (CP) scenario, and the ecological protection (EP) scenario) by coupling the FLUS and InVEST models. Our aim is to provide a scientific basis for optimizing urban land use structures and improving ecosystem service value.

2. Data Sources and Research Methods

2.1. Overview of the Study Area

Changchun is the capital of Jilin Province and is located at 43°05′ N–45°15′ N and 124°18′ E–127°05′ E (Figure 1). It is located in the mid-latitude area of the Northern Hemi-

sphere and has a temperate continental monsoon climate. The annual average temperature and the annual average precipitation are 4.8 °C and 522–615 mm, respectively. It has a flat terrain with an altitude of 250–350 m, which is suitable for agriculture. Changchun is one of the most important industrial cities in the northeast of China with a population of 9.07×10^6 and an area of 2.06×10^4 km^2. It is one of the main cities carrying out the strategy of revitalizing the old industrial bases in northeast China, which aims to accelerate the development of the northeastern regions.

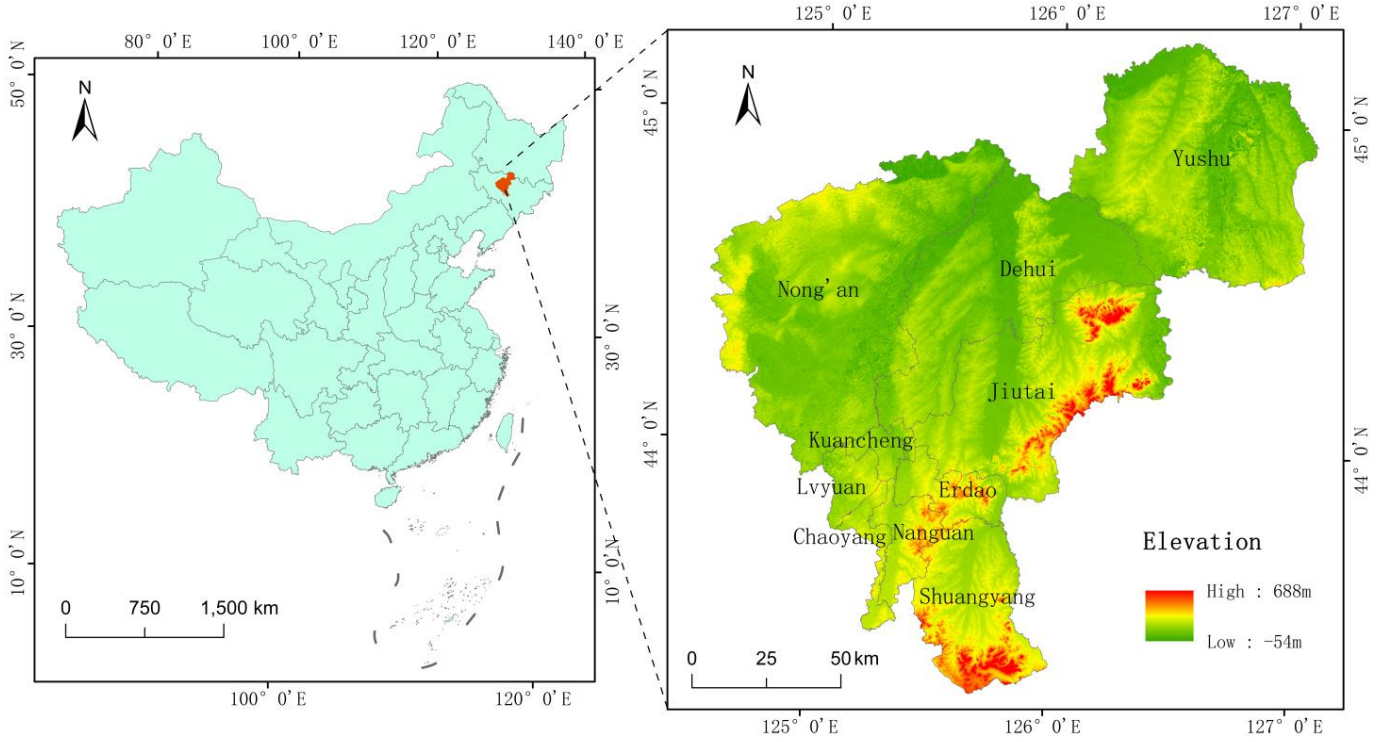

Figure 1. Diagram of the study area (Projected Coordinate System: Map of China: Krasovsky_1940_Albers; Map of Changchun: WGS_1984_UTM_Zone_52N).

2.2. Data Sources

The data used for future land use simulation mainly include land use, natural, and socioeconomic data (Table 1). The land use map of Changchun includes six land use types: cultivated land, forest, grassland, water bodies, construction land, and unused land. Land use maps from 2010 and 2020 and the distribution of gross domestic product (GDP) were obtained from the Resource and Environment Science Data Center of the Chinese Academy of Science [21], along with data on natural environmental factors including climate and terrain. Slope and aspect were extracted from the Digital Elevation Model (DEM) using ArcGIS10.6. Data on the city center, railway, and highway were obtained from the Changchun Natural Resources Bureau, along with restricted data including ecological redlines and permanent primary farmland. Distances were extracted by using Euclidean distance in ArcGIS10.6.

2.3. Research Method

2.3.1. The Research Framework

Based on land use data, we obtained the quantity of land use types under different scenarios in 2030 using the Markov model. With all the data prepared, we simulated land use patterns in 2030 under three scenarios using the FLUS model. Then, we estimated the carbon storage of Changchun during 2010–2030 based on the InVEST model. The research framework is shown as Figure 2.

Table 1. Data source.

Data Type	Data Name	Data Source
Land use	Land use maps of Changchun in 2010 and 2020	RESDCCAS [1]
Terrain factors	DEM	RESDCCAS
	Slope	Calculated using ArcGIS10.6
	Aspect	Calculated using ArcGIS10.6
Climate factors	Annual average temperature	RESDCCAS
	Annual average precipitation	RESDCCAS
Socioeconomic factors	GDP	RESDCCAS
	Distance to city center	CNRB [2]; Calculated using ArcGIS10.6
	Distance to railway	CNRB; Calculated using ArcGIS10.6
	Distance to highway	CNRB; Calculated using ArcGIS10.6
Restricted Data	Ecological redline	CNRB
	Permanent primary farmland	CNRB

[1] RESDCCAS represent Resource and Environment Science Data Center of Chinese Academy of Science [21].
[2] CNRB represent Changchun Natural Resources Bureau.

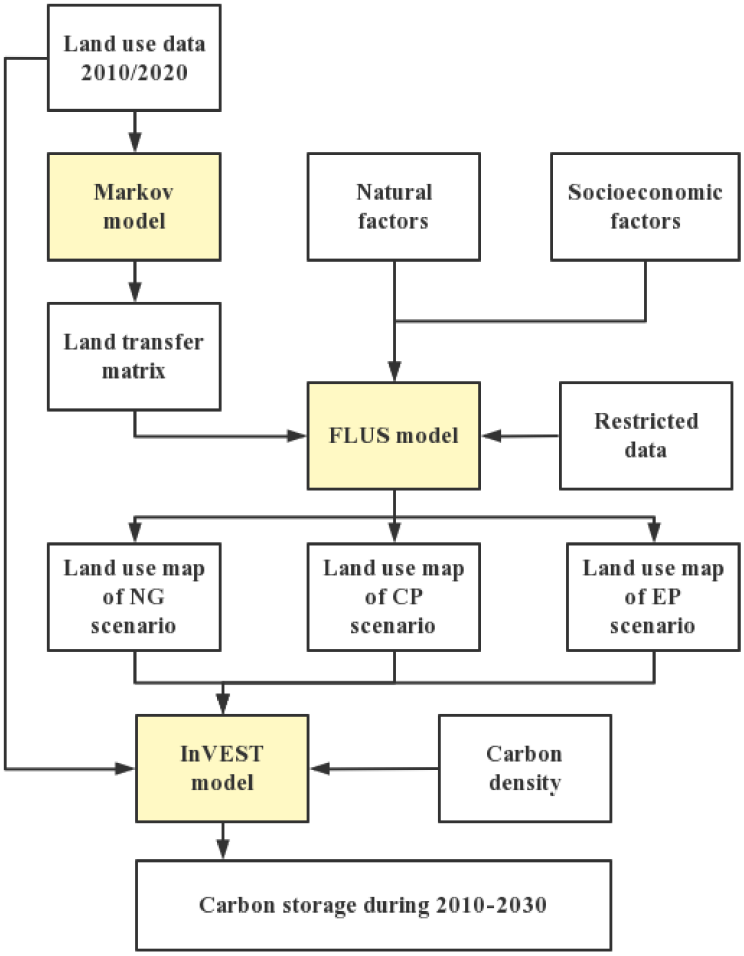

Figure 2. The research framework.

2.3.2. Defining Scenarios

It is necessary to consider multiple constraints in future land use simulation. We adjusted the transfer probability, intensity, and direction between different land use types and set parameters to reflect development under multi-scenario simulations. We set three scenarios by combining land use needs with urban planning.

(1) Natural growth (NG) scenario: As the basis of the other scenarios, this scenario is based on the transfer probability matrix of land use in Changchun from 2010 to 2020 without considering local policies and planning. With economic and technological development, converting construction land into other land use types is becoming impossible to achieve, so we set the corresponding value in the cost matrix to 0.

(2) Cultivated land protection (CP) scenario: This scenario was aimed at protecting cultivated land. We modified the transfer probability matrix in the Markov model on the basis of the NG scenario. The probability of transferring cultivated land to construction land is reduced by 60% and the probability of transferring cultivated land to unused land is set to 0. Cultivated land is not allowed to be converted into other land use types in this scenario. We added permanent primary farmland into the FLUS model as restricted data.

(3) Ecological protection (EP) scenario: This scenario aimed to strengthen the protection of ecological land such as forests, grasslands, and water bodies. The probability of transferring forest and grassland to construction land is reduced by 50%, the probability of converting water bodies to construction land is decreased by 10%, and forest, grassland, and water bodies are forbidden from being converted to unused land. The probabilities of transferring cultivated land to construction land and transferring cultivated land to forest are reduced by 35%. Forests and water bodies are not allowed to be converted into other land use types. Grassland can be transferred to forest and water bodies but not to other land use types. Additionally, ecological redlines were taken into consideration in the FLUS model.

The Markov model is a method of predicting the occurrence probability of events. It assumes that the current state is only related to the state at the previous moment but has nothing to do with other factors. It predicts the amount of future land use types according to a land use transfer probability matrix. The formula is as follows:

$$S_{(t+1)} = P_{ij} \times S_{(t)} \quad (1)$$

where $S_{(t)}$ and $S_{(t+1)}$ denote the land use states in the study area at moments t and t+1, respectively, and P_{ij} is the land use transfer probability matrix.

2.3.3. FLUS Model

The FLUS model introduces an artificial neural network (ANN) to construct transformation rules on the basis of the cellular automata (CA) model, which has the advantage of coupling human and natural activities to allow for higher accuracy [22]. The FLUS model is composed of an artificial neural network (ANN) and an adaptive inertia competition mechanism.

(1) Suitability probability calculation based on an artificial neural network

The ANN includes input, hidden, and output layers, and the optimal results are achieved by continuously updating the weight coefficients between the layers through a back propagation algorithm, which has the advantage of being able to learn and fit the complex relationship between the input data and the training target through multiple iterations [23,24]. It is an effective tool for iterating, adjusting, and fitting the relationship between the input data and the training target through learning–recall [25].

$$p(d,k,t) = \sum_j w_{j,k} \times \text{sigmoid}\left(\text{net}_j(d,t)\right) = \sum_j w_{j,k} \times \frac{1}{1+e^{-\text{net}_j(d,t)}} \quad (2)$$

where $p(d,k,t)$ denotes the adaptive probability of land use type k at moment t on element d, $w_{j,k}$ is an adaptive weight between the output layer and the hidden layer, $\text{net}_j(d,t)$ denotes the signal received by neuron j in the hidden layer, and sigmoid is the activation function of the connection between the input layer and the hidden layer. The hidden layer of the neural network is set to 12 in this paper.

(2) Self-adaptive inertia and competition mechanism

Based on a roulette selection mechanism, this mechanism incorporates the spatial computing function of CA and the self-adaptive inertia competition mechanism adjusts the land quantity and the land use demand to reach the target value, which can crack the uncertainty and complexity of mutual transformation in land use types [26]. The inertia coefficient is the core of the self-adaptive inertia competition mechanism, and the final simulation results not only depend on the probability of land distribution obtained from the neural network but are also subject to constraints such as neighborhood and conversion costs, reflecting the competition pattern of interactions in land use type changes [27]. The inertia coefficient is as follows:

$$\text{Inertia}_k^t = \text{Intertia}\begin{cases} \text{Inertia}_k^{t-1}, \text{if}\left|S_k^{t-1}\right| \le \left|S_k^{t-2}\right| \\ \text{Inertia}_k^{t-1} \times \frac{S_k^{t-1}}{S_k^{t-1}}, \text{if}\left|S_k^{t-1}\right| \le \left|S_k^{t-2}\right| < 0 \\ \text{Inertia}_k^{t-1} \times \frac{S_k^{t-1}}{S_k^{t-2}}, \text{if } 0 < \left|S_k^{t-2}\right| \le \left|S_k^{t-1}\right| \end{cases} \quad (3)$$

where Intertia$_k{}^t$ is the adaptive inertia coefficient of land use type k at moment t and $S_k{}^{t-1}$ and $S_k{}^{t-2}$ represent the differences between the demand of land use type k and the current land quantity at moments $t-1$ and $t-2$, respectively.

After the total probability of each raster is calculated, the final integrated suitability probability is calculated as:

$$TP_{d,k}^t = p(d,t,k) \times \Omega_{d,k}^t \times \text{Inertia}_k^t \times (1 - sc_{c \to k}) \quad (4)$$

where: $TP^t{}_{d,k}$ is the probability of element d becoming land use type k at moment t; $p(d,k,t)$ is the suitability probability of land use type k at moment t on element d; $\Omega^t{}_{d,k}$ denotes the neighborhood action; $sc_{c \to k}$ denotes the transfer cost of converting the original land use type c to land use type k, and 1-$sc_{c \to k}$ denotes the difficulty of land use type conversion occurring

$$\Omega_{d,k}^t = \frac{\Sigma_{N \times N}\text{con}\left(c_d^{t-1} = k\right)}{N \times N - 1} \times W_k \quad (5)$$

where $\sum_{N \times N}$con($c_d{}^{t-1}$=k) is the total number of rasters of land use type k at the end of the last iteration in the Moore neighborhood window of $N \times N$ and W_k is the weight of land use type k in the neighborhood role. The neighborhood factor weight indicates the expansion intensity of the land use type with parameters ranging from 0 to 1. A value close to 1 indicates strong expansion ability of the land use type [28]. The neighborhood factor weights according to the actual situation are shown in the table below (Table 2).

Table 2. Neighborhood factor weight (W_k).

Land Use Type	Cultivated Land	Forest	Grassland	Water Body	Construction Land	Unused Land
Neighborhood Factor Weight	0.7	0.6	0.5	0.5	1.0	0.5

The cost matrix indicates whether the conversion of land use types is allowed. We set the corresponding value to 0 when the conversion is allowed, while setting to 1 means that the conversion is forbidden. The cost matrix of the scenarios is set out in Table 3:

Table 3. Cost matrix.

	NG Scenario						CP Scenario						EP Scenario					
Land Use Type *	1	2	3	4	5	6	1	2	3	4	5	6	1	2	3	4	5	6
Cultivated Land	1	1	1	1	1	1	1	0	0	0	0	0	1	1	1	1	1	1
Forest	1	1	1	1	1	1	1	1	1	1	1	1	0	1	0	0	0	0
Grassland	1	1	1	1	1	1	1	1	1	1	1	1	0	1	1	1	0	0
Water Body	1	1	1	1	1	1	1	1	1	1	1	1	0	0	0	1	0	0
Construction Land	0	0	0	0	1	0	0	0	0	0	1	0	0	0	0	0	1	0
Unused Land	1	1	1	1	1	1	1	1	1	1	1	1	1	1	1	1	1	1

* 1, 2, 3, 4, 5, 6 represent cultivated land, forest, grassland, water body, construction land, and unused land respectively.

2.3.4. InVEST Model

The InVEST model aims to weigh the relationship between land use and ecosystem service functions [29], and it has been widely used to estimate carbon storage [30,31]. Carbon storage in terrestrial ecosystems mainly includes four basic carbon pools: above-ground biomass, below-ground biomass, soil organic carbon, and dead organic matter. The model combines land use data with the average carbon density of each land use type to estimate the total ecosystem carbon storage. Meanwhile, the impact of land use change on the carbon storage of the terrestrial ecosystem under various scenarios is quantitatively evaluated. The calculation of carbon storage can be expressed as follows:

$$C_i = C_{i\_above} + C_{i\_below} + C_{i\_soil} + C_{i\_dead} \quad (6)$$

$$C_{total} = \sum_{i=1}^{n} C_i \times A_i \quad (7)$$

where C_i is the average carbon density of land use type i, C_{i_above} is the above-ground vegetation carbon density of land use type i, C_{i_below} is the below-ground vegetation carbon density of land use type i, C_{i_soil} is the soil carbon density of land use type i, C_{i_dead} is the carbon density of dead organic matter, C_{total} denotes the total carbon storage of the study area, and A_i is the area of land use type i.

Since the content of dead organic matter carbon storage is very low and difficult to obtain, it is not considered in this paper for the time being. According to Chen et al. [32], Giardina et al. [33], and Alam et al. [34], biomass carbon density and soil carbon density have a significant linear correlation with climate factors. The models on the relationship between carbon density and annual average temperature and annual average precipitation, respectively, are as follows:

$$C_{BP} = 6.798e^{0.0054MAP} \ (R^2 = 0.70) \quad (8)$$

$$C_{BT} = 28MAT + 398 \ (R^2 = 0.47, P < 0.01) \quad (9)$$

$$C_{SP} = 3.3968MAP + 39996.1 \ (R^2 = 0.11) \quad (10)$$

where C_{BP} and C_{BT} denote the biomass carbon density calculated from average annual precipitation and average annual temperature, respectively; C_{SP} denotes the soil carbon density; MAP is the annual average precipitation; and MAT denotes the annual average temperature.

The carbon density correction factor equations are as follows.

$$K_{BP} = \frac{C'_{BP}}{C''_{BP}};\ K_{BT} = \frac{C'_{BT}}{C''_{BT}};\ K_B = K_{BP} \times K_{BT} = \frac{C'_{BP}}{C''_{BP}} \times \frac{C'_{BT}}{C''_{BT}} \quad (11)$$

$$K_S = \frac{C'_{SP}}{C''_{SP}} \quad (12)$$

where K_{BP} is the biomass carbon density precipitation factor correction factor, K_{BT} denotes the biomass carbon density temperature factor correction factor, K_B denotes the biomass carbon density correction factor, and K_S denotes the soil carbon density correction factor. C' denotes the data from Changchun, while C'' denotes the data from China or Jiangsu province.

We obtained the vegetation and soil carbon density data of the cultivated land, forests, and grassland of China from the research by Li et al. [35]. Vegetation carbon density is divided into above-ground biomass carbon density and below-ground biomass carbon density. According to the ratios of above-ground biomass to below-ground biomass of different kinds of vegetation [36–38], the above-ground and below-ground biomass carbon densities of cultivated land, forests, and grassland in China were calculated. We obtained the above-ground biomass carbon density of water bodies, construction land, and unused land in China from the research by Chen et al. [39] and the soil carbon density of water bodies, construction land, and unused land in Jiangsu Province from Chuai et al. [40]. The carbon densities of the below-ground biomass of water bodies, construction land, and unused land were defaulted to 0 according to Zhu et al. [1]. The annual average temperature of China, Jiangsu province, and Changchun City are 9 °C, 15.7 °C, and 4.8 °C, respectively. Additionally, the annual average precipitation in these areas is 628 mm, 1040.4 mm and 570.3 mm, respectively [1]. Finally, using formulas 8, 9, 10, 11, and 12, we calculated the carbon density of land use types in Changchun (Table 4).

Table 4. Carbon density of different land use types (Mg/hm^2).

Land Use Type	C_{i_above}	C_{i_below}	C_{i_soil}
Cultivated Land	2.88	0.54	104.93
Forest	35.31	7.69	184.70
Grassland	0.28	1.76	96.71
Water Body	0.18	0.00	63.90
Construction Land	0.15	0.00	57.52
Unused Land	0.08	0.00	58.78

3. Results and Analysis

3.1. Multi-Scenario Simulation for Future Land Use and Carbon Storage Estimation

The driving factors used for future land use simulation included DEM, slope, aspect, annual average temperature and precipitation, GDP, distance to city center, and railways and highways. The terrain of Changchun is high in the east and south. Most areas are flat. The distribution of annual average temperature is related to the terrain, and the temperature is lower in places with high terrain. Affected by the monsoon, the annual average precipitation is high in the east and low in the west. The municipal districts are located in the southwest, where the GDP is much higher than that of other counties. The administrative centers of districts and counties are shown as large patches of construction land in land use maps. According to the distance to highways and railways, the traffic condition in the southwest of Changchun was better than in other areas.

Based on a land use data map from 2010 and nine driving factors, we simulated the spatial distribution of land use types in 2020 using the FLUS model (Figure 3). We used the kappa coefficient to test the accuracy of the model. Our research showed that when the kappa coefficient is greater than 0.75, the simulation accuracy is reliable and has statistical significance [24]. Compared with the actual land use map of 2020, the overall accuracy of the FLUS model was 91.07%, and the Kappa coefficient was 77.43%, which means a high consistency. Therefore, it is credible to simulate future land use patterns based on the FLUS model. We modified the transfer probability matrix of land use from 2010 to 2020 to obtain quantities of land use types in 2030 under three scenarios. Figure 3 shows the

multi-scenario simulation for future land use under three scenarios in 2030. Under the NG scenario, urban expansion is evident, especially in the southwest of Changchun. Under the CP scenario, meanwhile, the expansion of construction land has been suppressed and cultivated land is well-preserved. It can be seen from the figure that the forest area has increased significantly under the EP scenario.

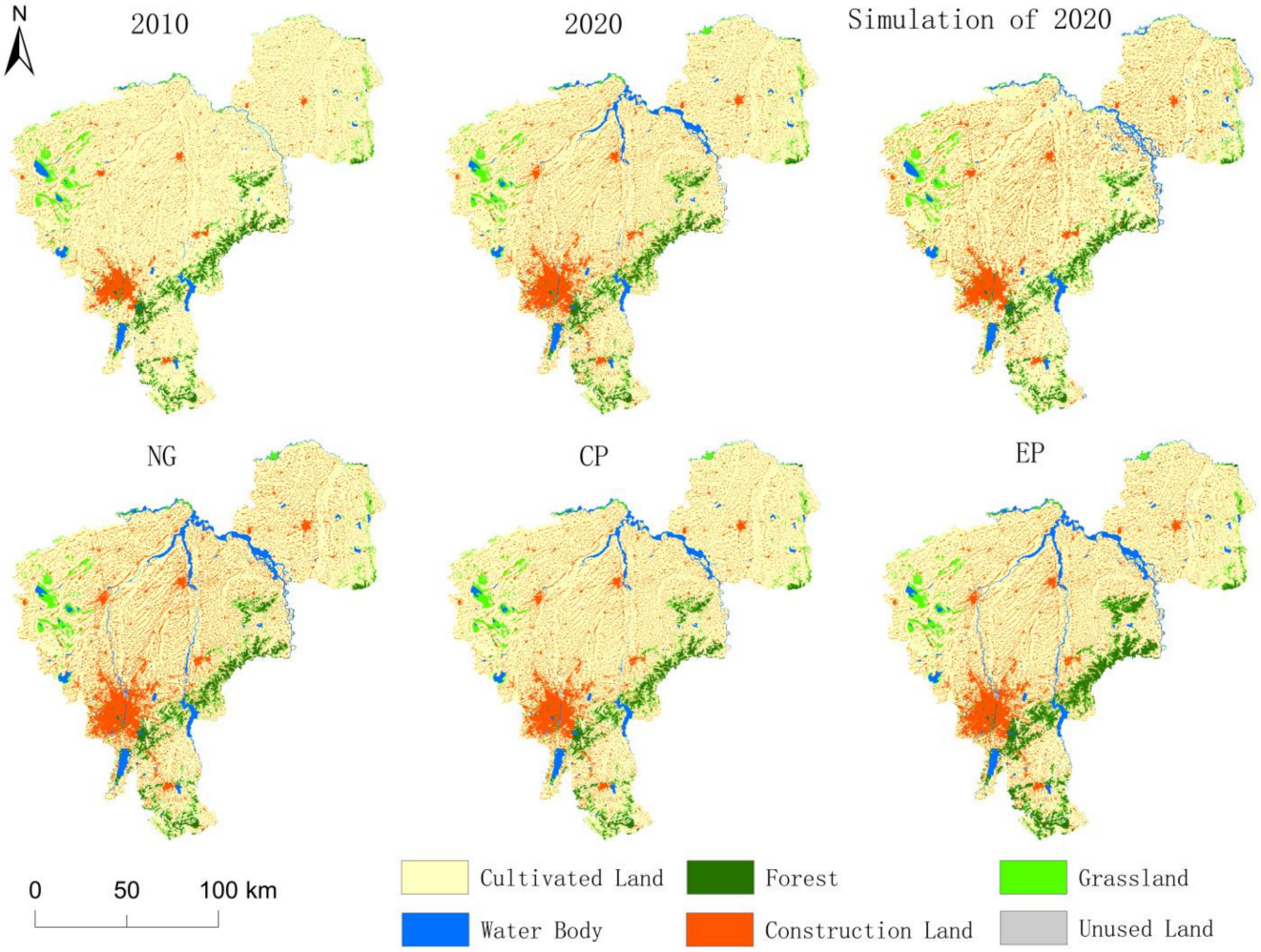

Figure 3. Land use map in 2010, 2020, simulation for 2020, and simulation under three scenarios for 2030 of Changchun.

From Table 4 we can see that the order of carbon density from high to low is forest, cultivated land, grassland, water, unused land, and construction land. By inputting carbon density data and land use data into the InVEST model, we estimated carbon storage in 2010 and 2020 and potential carbon storage under three scenarios in 2030 (Figure 4).

3.2. Impact of Land Use Change on Carbon Storage from 2010 to 2020

In the past decade, the carbon storage of terrestrial ecosystems in Changchun has shown a downward trend, with carbon storage falling from 2.22×10^8 Mg in 2010 to 2.16×10^8 Mg in 2020. The average carbon density was 107.68 Mg/hm^2 and 104.87 Mg/hm^2, respectively, exhibiting a reduction of 2.81 Mg/hm^2. Total carbon storage has been reduced by 5.81×10^6 Mg and the average annual reduction rate was 0.26%. From the perspective of spatial distribution, carbon storage of high value was generally distributed in the southeast of Changchun and that of the central part was lower (Figure 5). Areas with high carbon storage were concentrated in forests, which had a carbon density of 227.70 Mg/hm^2. The second-lowest carbon storage areas were mainly concentrated in cultivated land and

grassland. The carbon density in these areas was higher than 98.75 Mg/hm^2 and lower than 108.35 Mg/hm^2. The lowest carbon storage areas were concentrated in water bodies, construction land, and unused land. All the carbon storage values in these areas were lower than 64.08 Mg/hm^2.

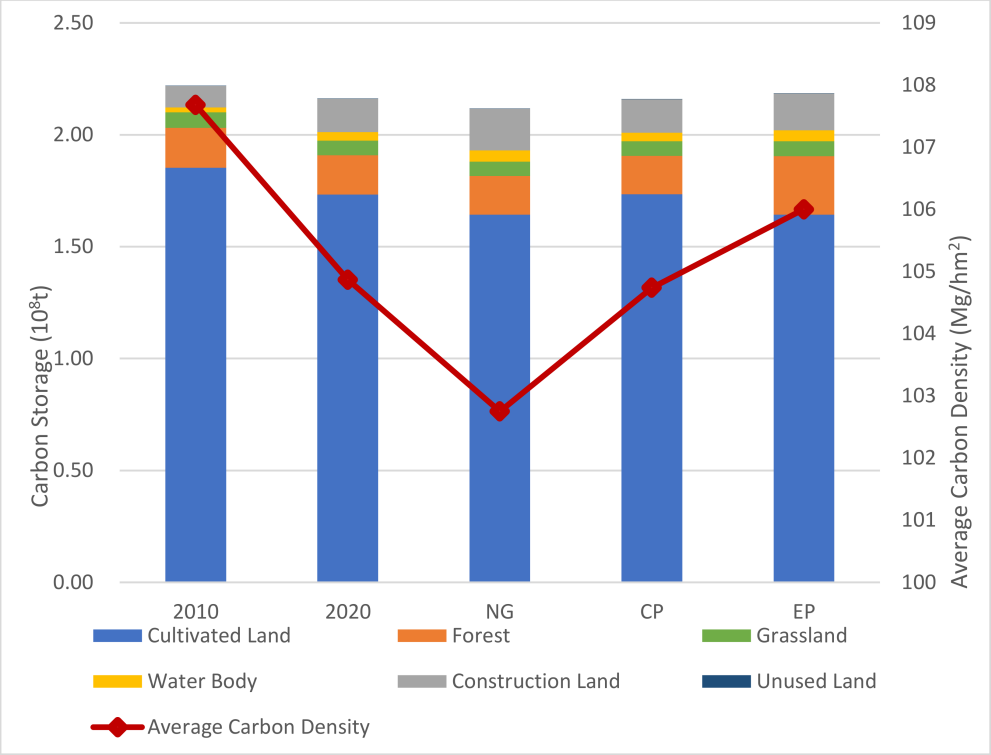

Figure 4. Carbon storage and average density in 2010, 2020, and under three scenarios in 2030.

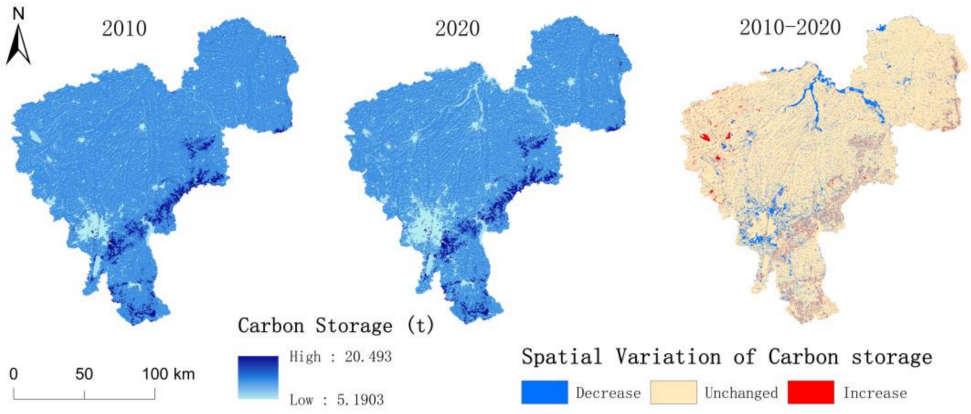

Figure 5. Spatial distribution and variation of carbon storage in Changchun from 2010 to 2020.

The characteristics of land use changes in Changchun from 2010 to 2020 were that the area of cultivated land in Changchun City decreased significantly, while the area of construction land and water bodies increased. This reflects an obvious characteristic of urban expansion. Cultivated land has always been the main land type, which is widely distributed in various regions of Changchun City, especially in the central and northern regions, accounting for about 80% of the total area of Changchun City. Over the past 10 years, the area and proportion of cultivated land have decreased by 1106.81 km^2 and 5.37%, respectively. This has caused a carbon loss of 1.20×10^7 Mg. The second is most common land use type is construction land, with an area of 2590.30 km^2 in 2020, accounting

for 12.57%, which is 905.73 km^2 (4.40%) higher than in 2010. This land use type if mainly distributed in the municipal districts of southwestern Changchun and the built-up areas of counties. From 2010 to 2020, the expansion of construction land was enhanced by rapid urban development, and a large area of cultivated land was converted to construction land. The carbon storage around the city center in the southwest of Changchun was significantly reduced, as well as that of the built-up areas of various counties. Forests generally extend along the northeast–southwest direction and are distributed along Dahei mountain, with an area of 772.80 km^2 in 2020, accounting for 3.75% of total land area. Grassland is mainly distributed around forests and water bodies. The carbon sequestration increased slightly in the western part due to the conversion of water bodies into grassland. The carbon storage in the Yinma River and Songhua River Basin decreased due to an increase in the water bodies. The area of unused land is small and accounts for only 0.03% of the total area. The area of woodland, grassland, and unused land decreased by 12.21 km^2 (0.06%), 36.75 km^2 (0.17%), and 0.34 km^2 (0.00%), respectively, between 2010 and 2020, which caused carbon losses of 2.78 $\times$ 10^5 Mg, 3.63 $\times$ 10^5 Mg, and 2.88 $\times$ 10^3 Mg, respectively. Some of these losses were offset by the increase in water body and construction land areas.

By overlaying the land use map in 2010 with the land use map in 2020 in ArcGIS10.6, we obtained the land use transfer matrix for 2010–2020 (Table 5). According to the land use transfer matrix, there were mutual conversions among various land use types in Changchun City. The area of cultivated land transferred into other types was 1686.89 km^2, which was about three times the area of other types transferred into cultivated land (580.07 km^2). The area of construction land transferred into other types (1266.08 km^2) was about four times the area of other types transferred into construction land (320.34 km^2). The transfer of cultivated land to construction land has been the main land use type conversion over the past decade, which led to most of the carbon storage loss. A total of 1181.40 km^2 of cultivated land was converted to construction land in 2010–2020, causing carbon losses of 5.99 $\times$ 10^6 Mg. This was mainly due to urban expansion. The area transferred from forests was mainly turned into grassland (101.30 km^2), with some also being transferred to cultivated land. Grassland ecosystems have lower stability than forest ecosystems, so grassland is easy to convert into or from other land use types. The transferred-in area of water (314.14 km^2) was significantly larger than the transferred-out area (63.61 km^2). The main source was cultivated land (279.88 km^2) and the carbon loss caused by conversion was 1.24 $\times$ 10^6 Mg.

Table 5. Land use transfer matrix in Changchun during 2010–2020 (km^2).

Land Use Type	Cultivated Land	Forest	Grassland	Water Body	Construction Land	Unused Land	Sum	Transferred-Out Area
Cultivated Land	15,413.09	95.88	129.50	279.88	1181.40	0.23	17,099.97	1686.89
Forest	83.75	584.17	101.30	4.08	11.55	0.16	785.01	200.84
Grassland	160.66	88.39	385.95	27.21	29.75	3.56	695.52	309.57
Water Body	24.47	1.00	34.91	276.59	3.20	0.02	340.20	63.61
Construction Land	311.06	3.06	3.44	2.76	1364.22	0.01	1684.57	320.34
Unused Land	0.12	0.29	3.67	0.20	0.19	2.29	6.75	4.46
Sum	15,993.16	772.80	658.77	590.73	2590.30	6.26	20,612.01	2585.70
Transferred-in Area	580.07	188.62	272.82	314.14	1226.08	3.98	2585.70	

3.3. Potential Impact of Land Use Change on Carbon Storage from 2020 to 2030

The potential spatial distribution and variation of carbon storage under three scenarios in 2030 are shown in Figures 6 and 7, respectively. It was estimated that the total carbon storage would be 2.12 $\times$ 10^8 Mg under the NG scenario, which is 4.36 $\times$ 10^6 Mg less than in 2020 (a decrease of 2.02%). The average carbon density was 102.75 Mg/hm^2. In this scenario, the land use pattern would tend to be stable. The expansion of construction land would still be serious, and it would occupy cultivated land and forests, which have higher carbon densities. The cultivated land around the heart of the city would be more likely to be converted to construction land in the future, and the aggregation of patches in the built-up areas would also increase. Every county would experience different degrees of decline

in carbon storage, especially those with a large area of cultivated land in the northern regions of Changchun such as Nong'an, Jiutai, Dehui, and Yushu. They exhibit a more serious reduction in carbon storage than other counties. Comparatively, the decrease in carbon storage was significantly weakened under the CP scenario. The spatial distribution pattern of carbon storage does not change significantly. The total carbon storage would be 2.16×10^8 Mg, which is 2.60×10^5 Mg less than in 2020 (a decrease of 0.12%), and the average carbon density would decrease by 0.13 Mg/hm^2, which indicates that carbon storage in the construction land protection scenario remains basically unchanged. As the main land use type of Changchun, cultivated land plays an important role in the carbon storage of the terrestrial ecosystem. In the EP scenario, the carbon storage of the terrestrial ecosystem would increase due to an increase in ecological land area. Forests, grassland, and water bodies would be protected in this scenario. The carbon storage and average carbon density would be 2.18×10^8 Mg and 106.00 Mg/hm^2, respectively, increasing by 2.33×10^6 Mg and 1.14 Mg/hm^2, respectively, compared with 2020. In terms of spatial distribution, the decrease in carbon storage due to the conversion of cultivated land into other land types would mainly be distributed in the northern region, while the areas with increased carbon storage would mainly be distributed around the Dahei Mountain and Shuangyang District. The reason for these reductions is the increase in forest area.

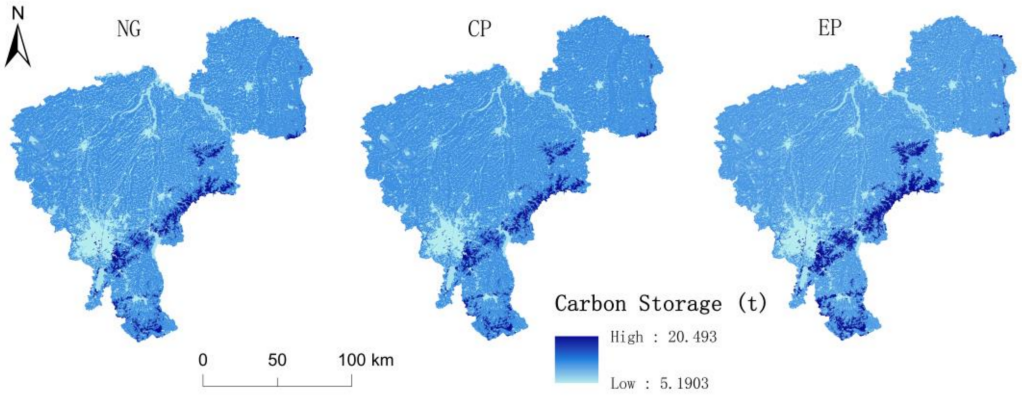

Figure 6. Potential spatial distribution of carbon storage under three scenarios in 2030.

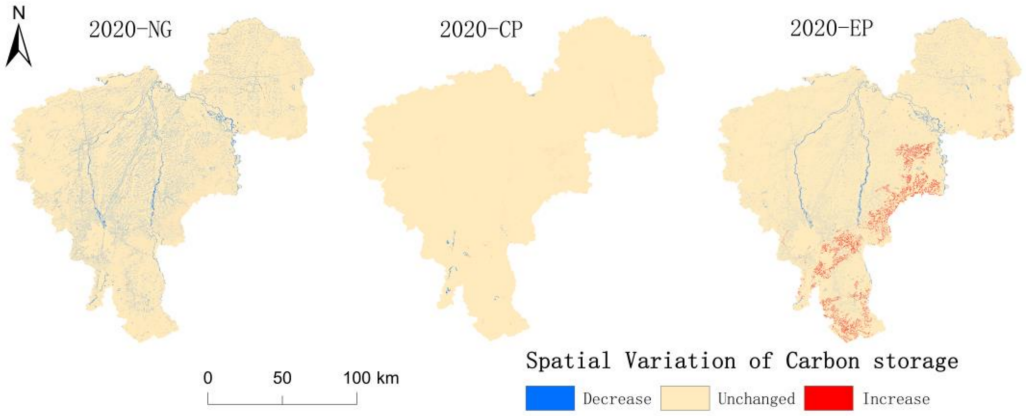

Figure 7. Potential spatial variation of carbon storage from 2020 to three scenarios in 2030.

The potential impact of land use change on carbon storage under various scenarios was quantitatively evaluated. Under the NG scenario, the carbon storage around the city center would decreased the most due to the expansion of construction land. The area and proportion of cultivated land under natural growth and ecological protection scenarios were 15,171.00 km^2 (73.60%), which decreased by 822.16 km^2 (3.99%) compared with 2020, causing a carbon storage decline with 8.91×10^6 Mg. Meanwhile, cultivated land

is well preserved, as is revealed by the fact that the area of cultivated land increased by 8.88 km^2 (0.06%) under the cultivated land protection scenario, which increased carbon storage by 9.62×10^4 Mg. The area of woodland and grassland was 755.20 km^2 (3.66%) and 655.71 km^2 (3.18%) under the NG and CP scenarios, respectively. The area of water under the NG scenario was 775.67 km^2 (3.76%), an increase of 184.95 km^2 (0.89%) compared with 2020. Under the cultivated land protection scenario, the area of water was only 601.58 km^2, accounting for 2.92% of land area, due to the control of cultivated land being transferred to other land use types. Forests, grassland, and water bodies, as ecological land, were effectively protected under the EP scenario. The area and proportion of forest land, grassland, and water were 1144.52 km^2 (5.55%), 673.17 km^2 (3.27%), and 776.86 km^2 (3.77%), respectively, which show increases of 371.73 km^2 (1.80%), 14.40 km^2 (0.07%), and 186.14.78 km^2 (0.90%), respectively, compared with 2020. The carbon storage or sequestration of forests, grassland, and water bodies increased by 8.46×10^6 Mg, 1.42×10^5 Mg, and 1.19×10^6 Mg, respectively. Construction land would still expand to a large extent under the NG scenario and may come to occupy other types of land that have higher carbon densities. The carbon storage of construction land increased by 3.79×10^6 Mg under the NG scenario, far less than the carbon loss of cultivated land. This would be controlled under the CP and EP. The expansion rate of construction land would be greatly slowed down under the CP and EP scenarios and the construction land area would increase by 0.96 km^2 and 249.60 km^2, respectively, compared with 2020. The total area of unused land is projected to increase by 0.25 km^2 under the NG scenario, while it would be developed and utilized under the CP and EP scenarios. The impact of unused land change on carbon storage was very small.

4. Discussion

4.1. Implications for Future Development Plan

About 90% of organic carbon in Changchun is stored in cultivated land and forests. Although the carbon density of cultivated land is lower than that of forests, the carbon storage of cultivated land accounts for more than 80% of the total carbon storage due to the large area of cultivated land, which shows the land uses type with larger areas and higher carbon densities have a greater influence on carbon storage. Forest cover is mainly found on the Dahei mountain range. The high altitude of the mountain determines the slope and aspect, limits the expansion of urban land, and occupies the dominant ecological niche in water conservation and forest resources [41]. It will remain an important carbon sink area in Changchun in the future, which is of great value for carbon balance and ecosystem stability over the whole city. Most of Changchun is located on the Songnen Plain, which is flat terrain that is suitable for human activities. Cultivated land is extensively distributed in the central and northern part of the city, and is greatly affected by human activities. Compared to areas with high forest coverage, the carbon storage in most areas of Changchun was maintained at a medium level. Low-density carbon storage was mainly distributed in the southwest of the city and in built-up areas. Although the carbon density of water is lower than that of cultivated land and grassland, the ecological service value of water is higher. Furthermore, the water area showed an increasing trend in all three scenarios, which is also one of the reasons for the loss of carbon storage. Urban carbon storage decline remains an inevitable problem under continuous urban expansion. It is worth thinking about how to slow down this decline in carbon storage. This paper showed the impact of land use change on carbon storage under several scenarios, which can provide a reference for urban sustainable development. With the proposal of the strategy of revitalizing the old industrial bases in northeast China, there are many cities experiencing different degrees of decline in carbon storage, including Changchun. Cultivated land plays an important role in carbon storage. It is equally important to protect cultivated land while protecting ecological land. The priority of a territorial development plan should be the overall improvement of the economic, social, and ecological benefits of land.

4.2. Limitations and Improvement

Our study has some limitations. The potential impact of land use on carbon density depends largely on the simulation of land use patterns. The Markov and FLUS models combine the advantages of quantity prediction and spatial distribution, and the accuracy of land use pattern simulation has been improved to a certain extent. However, land use change is a complex and dynamic process, and urban development is influenced by several of factors. In this paper, we considered nine driving factors in our model and simulated three scenarios: NG, CP, and EP. The more factors that are taken into account, the more accurate the results will be. The parameters set in the FLUS model are subjective and idealized. The Markov chain assumes that the current state is only related to the state at the previous moment, without considering long-term economic and social development's role in the current situation [10,42]. The demand area of land use types is calculated only by modifying the transfer probability matrix in the Markov model, which is less related to planning and policies in the study area, such as ecological protection redlines. In future research, we should take local planning into consideration in order to improve the accuracy of the models.

As for the source of carbon density, many scholars have collected carbon density data from papers in their study area or via experimental measurements. In regions with few research results it can be difficult to obtain comprehensive and complete data. Moreover, using multiple sources will affect the accuracy of the results. In order to improve the accuracy of carbon storage estimation in a terrestrial ecosystem, we used a carbon density correction method to calculate carbon density in this paper according to Zhu et al. [1]. It is fast and effective to use this method, but it also comes with uncertainties. Taking data of China as the basic data for carbon density correction, the present study was a detailed study within this context. Due to the vast area of China, the data need to be improved in the future. Biomass carbon density is mainly influenced by climate, terrain, nitrogen deposition, hydrological conditions, tree species composition, etc. Soil carbon density is mainly influenced by soil type, soil respiration rate, and vegetation cover [43]. Due to the difficulty of quantifying many of these factors, only temperature and precipitation were considered when correcting the carbon density in this paper. This should be improved in future research. As it is affected by human activities and climate change, the carbon density will change dynamically over time. Therefore, there is inherent uncertainty in estimations of carbon storage that use a fixed value of carbon density for different periods. In future research, we should verify the accuracy of carbon density through experimental measurements to improve the accuracy of the estimation results in the InVEST model.

4.3. Soil Carbon Pool

It can be seen from Table 4 that the carbon density of the soil is much higher than that of the vegetation. The soil carbon pool is the largest carbon pool in the terrestrial ecosystem, which is composed of organic carbon pools and inorganic carbon pools. Its carbon storage is three times that of atmospheric carbon pools and 3.8 times that of biological carbon pools [44]. The global soil organic carbon (SOC) is about 1550 Pg and the inorganic carbon (SIC) is about 750 Pg [45]. In the InVEST model, we only took soil organic carbon into consideration. According to Wu et al. [46], tillage measures can lead to a significant increase in inorganic carbon in the Songnen Plain. The significant impact of land use on soil inorganic carbon cannot be ignored [46–48]. In addition, the soil types in Changchun City mainly consist of dark brown soil, albic soil, black soil, black calcareous soil, and alluvial meadow soil. The soil carbon density varies by soil type. These factors should be taken into account in future studies.

5. Conclusions

Taking Changchun City in northeast of China as the study area, we combined the FLUS model with the Markov model to simulate land use patterns in 2030 under three scenarios (a natural growth scenario, a cultivated land protection scenario, and an ecological protec-

tion scenario) based on land use data from 2010 and 2020. Then, we assessed terrestrial ecosystem carbon storage over the past decade and over the next 10 years based on the carbon storage and sequestration module in the InVEST model. This paper estimates the impact of land use changes on carbon storage in terrestrial ecosystems under several scenarios in Changchun, which can provide a reference for urban sustainable development.

The results show that cultivated land plays an important role in carbon storage in Changchun. From 2010 to 2020, rapid urban development led to the expansion of construction land and a significant decrease in cultivated land. The transfer of cultivated land to construction land has been the main land use type conversion over the past decade, which led directly to most of the carbon storage loss. In the NG scenario, the counties with a large area of cultivated land in the northern regions would experience a more serious reduction in carbon storage than others. In the CP scenario, this situation would be greatly improved. In the EP scenario, the carbon storage would be increased due to the protection of ecological land. Cultivated land accounts for nearly 80% of the total area of Changchun. As for other cities with similar backgrounds and situations in northeast China, it is equally important to protect both cultivated land and ecological land. In the future, the priority of any territory development plan should be protecting existing resources, such as cultivated land and ecological land, while simultaneously comprehensively improving the economic, social, and ecological benefits of the land.

Author Contributions: Conceptualization, S.L. and Z.L.; Data curation, Z.L.; Formal analysis, Y.L.; Funding acquisition, S.L.; Methodology, Y.L.; Project administration, S.L.; Resources, Y.L. and S.L.; Software, X.L.; Supervision, S.L. and Z.L.; Validation, Y.L. and Z.L.; Visualization, Y.L. and X.L.; Writing—original draft, Y.L.; Writing—review & editing, S.L. and Z.L. All authors have read and agreed to the published version of the manuscript.

Funding: This research was funded by Natural Science Foundation of Jilin Province, China (Grant No. 20210101395JC).

Institutional Review Board Statement: Not applicable.

Informed Consent Statement: Not applicable.

Data Availability Statement: Not applicable.

Conflicts of Interest: The authors declare no conflict of interest.

References

1. Zhu, W.; Zhang, J.; Cui, Y.; Zheng, H.; Zhu, L. Assessment of territorial ecosystem carbon storage based on land use change scenario: A case study in Qihe River Basin. *Acta Geogr. Sin.* **2019**, *74*, 446–459.
2. Chen, Y.; Yue, W.; Liu, X.; Zhang, L.; Chen, Y. Multi-Scenario Simulation for the Consequence of Urban Expansion on Carbon Storage: A Comparative Study in Central Asian Republics. *Land* **2021**, *10*, 608. [CrossRef]
3. Liu, J.; Sleeter, B.M.; Zhu, Z.; Loveland, T.R.; Sohl, T.; Howard, S.M.; Key, C.H.; Hawbaker, T.; Liu, S.; Reed, B.; et al. Critical land change information enhances the understanding of carbon balance in the United States. *Glob. Change Biol.* **2020**, *26*, 3920–3929. [CrossRef] [PubMed]
4. Mendoza, P.A.; Corona, N.R.; Kraxner, F.; Leduc, S.; Patrizio, P. Identifying effects of land use cover changes and climate change on terrestrial ecosystems and carbon stocks in Mexico. *Glob. Environ. Change* **2017**, *53*, 12–23.
5. Liu, X.; Li, X.; Liang, X.; Shi, H.; Ou, J. Simulating the Change of Terrestrial Carbon Storage in China Based on the FLUS-InVEST Model. *Trop. Geogr.* **2019**, *39*, 397–409.
6. Eigenbrod, F.; Bell, V.A.; Davies, H.N.; Heinemeyer, A.; Armsworth, P.R.; Gaston, K.J. The impact of projected increases in urbanization on ecosystem services. *Proc. Biol. Sci.* **2011**, *278*, 3201–3208. [CrossRef] [PubMed]
7. Jia, H.X.; Wang, X.; Xiao, J.J.; Jang, S.L.; Li, J.; Shi, C.M.; Zhao, Y.F. Simulated soil organic carbon stocks in northern China's cropland under different climate change scenarios. *Soil Tillage Res.* **2021**, *213*, 105088. [CrossRef]
8. Liu, Y.; Zhang, J.; Zhou, D.; Ma, J.; Dang, R.; Ma, J.; Zhu, X. Temporal and spatial variation of carbon storage in the Shule River Basin based on InVEST model. *Acta Ecol. Sin.* **2021**, *41*, 4052–4065.
9. Shi, M.; Wu, H.; Jia, H.; Zhu, L.; Dong, T.; He, P.; Yang, Q. Temporal and spatial evolution and prediction of carbon stocks in Yili Valley based on MCE-CA-Markov and InVEST models. *J. Agric. Resour. Environ.* **2021**, *38*, 1010–1019.
10. Deng, Y.; Yao, S.; Hou, M.; Zhang, T.; Lu, Y.; Gong, Z.; Wang, Y. Assessing the effects of the Green for Grain Program on ecosystem carbon storage service by linking the InVEST and FLUS models: A case study of Zichang county in hilly and gully region of Loess Plateau. *J. Nat. Resour.* **2020**, *35*, 826–844.

11. Zhang, B.; Li, L.; Dong, J. Land use change and its impact on carbon storage under the constraints of "three lines": A case study of Wuhan City Circle. *Acta Ecol. Sin.* **2022**, *42*, 1–16.
12. Li, L.; Song, Y.; Wei, X.; Dong, J. Exploring the impacts of urban growth on carbon storage under integrated spatial regulation: A case study of Wuhan, China. *Ecol. Indic.* **2020**, *111*, 106064. [CrossRef]
13. He, C.; Zhang, D.; Huang, Q.; Zhao, Y. Assessing the potential impacts of urban expansion on regional carbon storage by linking the LUSD-urban and InVEST models. *Environ. Model. Softw.* **2016**, *75*, 44–58. [CrossRef]
14. Zhu, Z.; Ma, X.; Hu, H. Spatio-temporal evolution and prediction of ecosystem carbon stocks in Guang zhou City by coupling FLUS-InVEST models. *Bull. Soil Water Conserv.* **2021**, *41*, 222–229.
15. Wang, Y.; Luo, G.; Zhao, S.; Han, Q.; Li, C.; Fan, B.; Chen, Y. Effects of arable land change on regional carbon balance in Xinjiang. *Acta Geogr. Sin.* **2014**, *69*, 110–120.
16. Leonardo, C.; Josep, G.C.; Prabir, P.; Philippe, C.; Kazuhito, I.; Hanqin, T.; Masayuki, K.; Shilong, P.; Almut, A.; Anna, B.H.; et al. Regional carbon fluxes from land use and land cover change in Asia, 1980–2009. *Environ. Res. Lett.* **2016**, *11*, 074011.
17. Zhu, G.; Qiu, D.; Zhang, Z.; Sang, L.; Liu, Y.; Wang, L.; Zhao, K.; Ma, H.; Xu, Y.; Wan, Q. Land-use changes lead to a decrease in carbon storage in arid region, China. *Ecol. Indic.* **2021**, *127*, 107770. [CrossRef]
18. Chen, L.; Cai, H.; Zhang, T.; Zhang, X.; Zeng, H. Land use multi-scenario simulation analysis of Rao River Basin based on Markov-FLUS model. *Acta Ecol. Sin.* **2022**, *42*, 1–12.
19. Ke, X.; Tang, L. Impact of cascading processes of urban expansion and cropland reclamation on the ecosystem of a carbon storage service in Hubei Province, China. *Acta Ecol. Sin.* **2019**, *39*, 672–683.
20. Tang, L.; Ke, X.; Zhou, T.; Zheng, W.; Wang, L. Impacts of cropland expansion on carbon storage: A case study in Hubei, China. *J. Environ. Manag.* **2020**, *265*, 110515. [CrossRef]
21. Resource and Environment Science Data Center of the Chinese Academy of Science. Available online: https://www.resdc.cn (accessed on 10 January 2022).
22. Liu, X.; Liang, X.; Li, X.; Xu, X.; Ou, J.; Chen, Y.; Li, S.; Wang, S.; Pei, F. A future land use simulation model (FLUS) for simulating multiple land use scenarios by coupling human and natural effects. *Landsc. Urban Plan.* **2017**, *168*, 94–116. [CrossRef]
23. Li, X.; Anthony, G.Y. Neural-network-based cellular automata for simulating multiple land use changes using GIS. *Int. J. Geogr. Inf. Sci.* **2002**, *16*, 323–343. [CrossRef]
24. Li, J.; Gong, J.; Guldmann, J.; Li, S.; Zhu, J. Carbon Dynamics in the Northeastern Qinghai–Tibetan Plateau from 1990 to 2030 Using Landsat Land Use/Cover Change Data. *Remote Sens.* **2020**, *12*, 528. [CrossRef]
25. Ding, Q.; Chen, Y.; Bu, L.; Ye, Y. Multi-Scenario Analysis of Habitat Quality in the Yellow River Delta by Coupling FLUS with InVEST Model. *Int. J. Environ. Res. Public Health* **2021**, *18*, 2389. [CrossRef]
26. Lin, W.; Sun, Y.; Steffen, N.; Wang, Z. Scenario-based flood risk assessment for urbanizing deltas using future land-use simulation (FLUS): Guangzhou Metropolitan Area as a case study. *Sci. Total Environ.* **2020**, *739*, 139899. [CrossRef]
27. Wang, X.; Ma, B.; Li, D.; Chen, K.; Yao, H. Multi-scenario simulation and prediction of ecological space in Hubei province based on FLUS model. *J. Nat. Resour.* **2020**, *35*, 230–242.
28. Li, G. Land Use Change and Simulation in Shenzhen Based on FLUS Model. Master's Thesis, Wuhan University, Wuhan, China, May 2018.
29. Hu, W.; Li, G.; Gao, Z.; Jia, G.; Wang, Z.; Li, Y. Assessment of the impact of the Poplar Ecological Retreat Project on water conservation in the Dongting Lake wetland region using the InVEST model. *Sci. Total Environ.* **2020**, *733*, 139423. [CrossRef]
30. Liu, X.; Wang, S.; Wu, P.; Feng, K.; Hubacek, K.; Li, X.; Sun, L. Impacts of Urban Expansion on Terrestrial Carbon Storage in China. *Environ. Sci. Technol.* **2019**, *53*, 6834–6844. [CrossRef]
31. Zhao, M.; He, Z.; Du, J.; Chen, L.; Lin, P.; Fang, S. Assessing the effects of ecological engineering on carbon storage by linking the CA-Markov and InVEST models. *Ecol. Indic.* **2019**, *98*, 29–38. [CrossRef]
32. Chen, G.; Yang, Y.; Xie, J.; Du, Z.; Zhang, J. Total below ground carbon allocation in China's forests. *Acta Ecol. Sin.* **2007**, *27*, 5148–5157.
33. Giardina, C.P.; Ryan, M.G. Evidence that decomposition rates of organic carbon in mineral soil do not vary with temperature. *Nature* **2000**, *404*, 858–861. [CrossRef]
34. Alam, S.A.; Starr, M.; Clark, B.J.F. Tree biomass and soil organic carbon densities across the Sudanese woodland savannah: A regional carbon sequestration study. *J. Arid Environ.* **2013**, *89*, 67–76. [CrossRef]
35. Li, K.; Wang, S.; Cao, M. Vegetation and soil carbon storage in China. *Sci. Sin.* **2003**, *33*, 72–80. [CrossRef]
36. Fang, J.; Liu, G.; Xu, S. Biomass and net production of forest vegetation in China. *Acta Ecol. Sin.* **1996**, *16*, 497–508.
37. Huang, M.; Ji, J.; Cao, M.; Li, K. Modeling study of vegetation shoot and root biomass in China. *Acta Ecol. Sin.* **2006**, *26*, 4156–4163.
38. Piao, S.; Fang, J.; He, J.; Xiao, Y. Spatial distribution of grassland biomass in China. *Chin. J. Plant Ecol.* **2004**, *28*, 491–498.
39. Chen, L.; Liu, G.; Li, H. Estimating Net Primary Productivity of Terrestrial Vegetation in China Using Remote Sensing. *J. Remote Sens.* **2002**, *6*, 129–135.
40. Chuai, X.; Huang, X.; Zheng, Z.; Zhang, M.; Liao, Q.; Lai, L.; Lu, J. Land use change and its influence on carbon storage of terrestrial ecosystems in Jiangsu Province. *Resour. Sci.* **2011**, *33*, 1932–1939.
41. Shang, B. Study on the Influence of Land cover Change on Regional Ecosystem Services in Changchun City. Master's Thesis, Jilin University, Changchun, China, 2021.

42. Weng, Q. Land use change analysis in the Zhujiang Delta of China using satellite remote sensing, GIS and stochastic modelling. *J. Environ. Manag.* **2002**, *64*, 273–284. [CrossRef]
43. Huang, H. Reasearch on Land Use/Land Cover Change and Carbon Storage Based on InVEST Model. Master's Thesis, China University of Geosciences (Beijing), Beijing, China, 2015.
44. Zhang, X.B.; Li, X.; Xu, M.; Sun, N.; Shi, F. Vertical distribution of soil organic and inorganic carbon pools in soils of northern China and their relationship under different land use types. *J. Plant Nutr. Fertil.* **2020**, *26*, 1440–1450.
45. Zu, Y.G.; Li, R.; Wang, W.J.; Su, D.X.; Wang, Y.; Qiu, L. Soil organic and inorganic carbon contents in relation to soil physicochemical properties in northeastern China. *Acta Ecol. Sin.* **2011**, *31*, 5207–5216.
46. Wu, H.B.; Guo, Z.T.; Gao, Q.; Peng, C.H. Distribution of soil inorganic carbon storage and its changes due to agricultural land use activity in China. *Agric. Ecosyst. Environ.* **2008**, *129*, 413–421. [CrossRef]
47. Li, Z.P.; Han, F.X.; Su, Y.; Zhang, T.L.; Sun, B.; Monts, D.L.; Plodinec, M.J. Assessment of soil organic and carbonate carbon storage in China. *Geoderma* **2006**, *138*, 119–126. [CrossRef]
48. Mi, N.; Wang, S.Q.; Liu, J.Y.; Yu, G.R.; Zhang, W.J.; Jobbagy, E. Soil inorganic carbon storage pattern in China. *Glob. Change Biol.* **2008**, *14*, 2230–2387. [CrossRef]